Proceedings of the 2006 IEEE/RSJ
International Conference on Intelligent Robots and Systems
October 9 - 15, 2006, Beijing, China

Kinematic Design Optimization of an Actuated Carrier for the DLR Multi-Arm Surgical System

Rainer Konietschke, Tobias Ortmaier,
Ulrich Hagn, and Gerd Hirzinger
Institute of Robotics and Mechatronics
German Aerospace Center (DLR)
D-82234 Weßling, Germany
Email: Rainer.Konietschke@dlr.de

Silvia Frumento
University of Genova, PMARLab, DIMEC
Via all'Opera Pia, 15/A
16145 Genova, Italy

***Abstract*— In this paper, a generic approach to optimize the design of an actuated carrier for the DLR multi-arm surgical system is presented. The carrier is attached to the ceiling of the operating room and provides additional degrees of freedom to the surgical robots with the purpose of automatic, optimal positioning of their bases as well as guaranteeing high stiffness. Standard workspaces of minimally invasive as well as open surgical procedures are considered and optimization criteria are derived. The minimum necessary degrees of freedom of the carrier are obtained as well as the optimal segment dimensions by use of an optimization with genetic algorithms.**

I. Introduction

As opposed to the majority of today's robotic applications in industry, where the trajectories of the (possibly collaborating) robots are known in advance, in telemanipulation applications with multiple robots the same workspace is shared and the robot motion is commanded in real-time by the operator. Usually, the operator is interested only in commanding the instruments (attached to the robots), whereas the robotic system itself should be the enabling agent operating in the background. However, performance constraints introduced by the robotic system such as singular configurations, boundaries of the workspace and collisions can occur and have to be avoided if possible. Particularly in direct human interaction, and even more in surgical robotics, safe operation of the system inside the designated workspace has to be guaranteed. Careful planning of the intervention, including e.g. optimal positioning of the robot bases, can help to lower the risk of performance reductions. To position the robotic system according to the results of the preoperative, patient specific planning, a positioning device is necessary that provides a sufficient number of degrees of freedom (DoF). This contribution describes a systematic approach to determine a kinematically optimal design for an actuated carrier to automatically position up to three DLR medical arms *KineMedic* as described in [1] (see Fig. 1) in interventions covering both (telemanipulated) minimally invasive, robotic surgery (MIRS) and operations in open surgery.

The next section develops, starting from current practice in MIRS, potential improvements of the positioning of medical robots in the operating room (OR). Sect. III describes the chosen procedure to obtain an optimized design for the positioning device and Sect. IV shows some favored design alternatives. A conclusion with further possible developments is given in Sect. V.

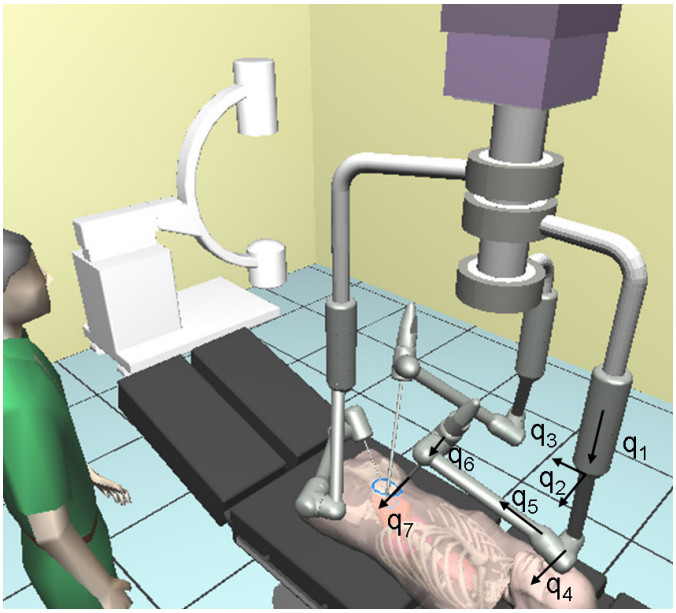

Fig. 1. The DLR medical operating scenario with three KineMedics disposing of 7 joints $\mathbf{q}^{\mathrm{T}} = (q_1, ..., q_7)^{\mathrm{T}}$ each, mounted to an actuated carrier.

II. State of the Art

The OR is a remarkably ill-suited environment for robots. It is poorly structured, since the position of OR equipment is often changed during the intervention, the staff is moving and the patient itself is constantly in motion e.g. due to heartbeat and breathing. Naturally the safety requirements by far exceed those in industrial applications, where human interaction can be excluded in most cases. However, the potential advantage of combining skills of man with those of robots (see e.g. [1]) has let to a variety of propositions for robotic systems in the OR [2]. Especially the field of MIRS has proven to be a rewarding application area for robots, with about 400 $\mathrm{daVinci}^{\mathrm{TM}}$ systems of Intuitive Surgical currently installed [3]. In MIRS, robots carry long, thin instruments

1-4244-0259-X/06/$20.00 ©2006 IEEE

that reach the operating field inside the patient through small incisions, or ports, thus avoiding large incisions as needed in open surgery. The robots are teleoperated by a surgeon. Compared to minimally invasive surgery (MIS), where the surgeon is manipulating the instruments directly, the use of robots enables additional features such as e.g. motion scaling, tremor filtering, or multi robot control. A good positioning of the robotic system relative to the patient is crucial for a successful intervention to e.g. ensure that the volume of the operating field coincides with the (confined) robot workspace. Current systems however hardly provide any assistance in this step, and the OR staff is mainly supposed to position the OR equipment using visual judgment and experience. Approaches to optimally position e.g. the daVinci system are reported in [4] to be rather cumbersome. The kinematic design optimization of an actuated carrier, attached to the ceiling rather than the floor or table, is therefore discussed in this paper.

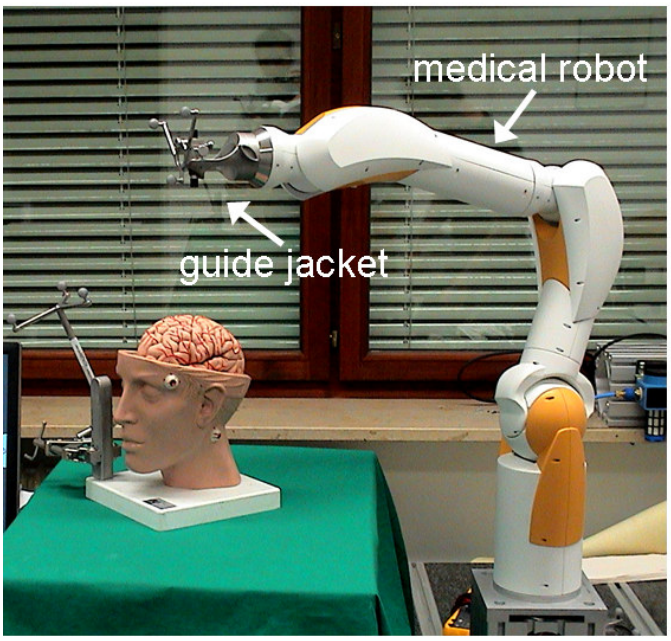

Fig. 2. First prototype of the DLR medical robot *KineMedic*. A guide jacket is attached to the tool tip to assist in positioning a biopsy needle.

III. Problem Statement

In the current study, the dimensions as well as the necessary actuators of a carrier to position up to three KineMedics at their optimal base positions are determined. The KineMedics have 7 DoF each as shown in Fig. 1. They can be equipped with articulated instruments with 2 DoF as described in [5], with a stereoscopic endoscope, or with other tools as e.g. a cutting tool. Fig. 2 shows the first prototype of the robot with a guide jacket attached to the tool tip for assisting in positioning a biopsy needle.

In this section, the considered operation scenarios are described, the optimization parameters are defined, and the procedure to evaluate design alternatives is shown.

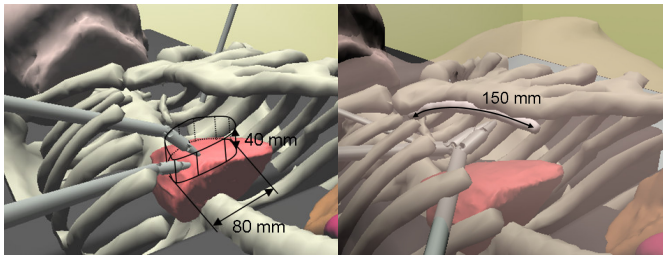

(a) Workspace in heart surgery. (b) Preparation of the LITA.

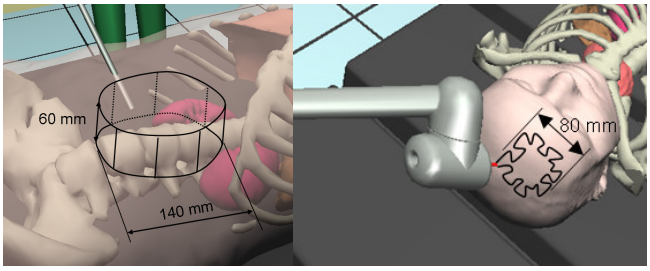

(c) Abdominal exploration. (d) Workspace in open surgery.

Fig. 3. Workspaces of the considered operation scenarios.

A. Operation Scenarios

The actuation and mounting setup should be able to deal with various operation scenarios as shown in Fig 3. The scenarios have been created using segmented CT data of real patients and correspond with earlier examinations of typical workspaces in surgical robotics [6]. Every workspace was varied both in size and distance to the skin surface to take into account 3 (significantly different) patient geometries. Acquisition of a larger patient database is desirable as future work (bearing in mind that coverage of the whole diversity in human anatomy is naturally not possible). The following operation scenarios are considered:

1) Operation on the heart: A workspace as shown in Fig. 3a is assumed. Two robots carry articulated instruments and a third robot carries a stereo endoscope. Inside the workspace, high dexterity and manipulability has to be guaranteed. Especially, requirements from the beating heart compensation as suggested in [7] have to be met.

2) Preparation of the left internal thoracic arteria (LITA): The medical robots dispose of similar instruments as in the previous scenario, the workspace is shown in Fig 3b. The preparation of the LITA represents a special category of tasks since the workspace is very spacious in one direction and located above the entry points into the human body.

3) Abdominal exploration: In this scenario (Fig. 3c), only the robot carrying the endoscope is involved. The robot has to position the endoscope throughout a large workspace to enable investigation of the whole abdominal cavity. Since the endoscope is not actuated inside of the patient, orientations

are not taken into consideration.

4) Open surgery: Additionally to [6], a workspace for open surgery, namely a cutting task on the human skull, is considered (see Fig. 3d). Applications in e.g. orthopedics can be performed by the system if the medical arm is equipped with a tailored cutting tool suitable for cutting bone.

Inside the workspaces, certain quality measures are evaluated, to ensure e.g. that the tool tips of the robots can move with at least 60 mm/s and $30°/s$ as needed for beating heart compensation and to ensure that the relative positioning accuracy is better than 0.1 mm and $0.5°$ to outperform human accuracy as measured e.g. in [8]. See Tab. I for all compulsory requirements.

TABLE I
COMPULSORY PERFORMANCE REQUIREMENTS

Requirement	Value
Distance from joint limits/singularities	$3°$
Minimum distance between robot structures	5 cm
Minimum translational tool tip velocity	60 mm/s
Minimum rotational tool tip velocity	$30°/s$
Relative translational tool tip accuracy	0.1 mm
Relative rotational tool tip accuracy	$0.5°$
Tool tip dexterity	$\pm 20°$

Every workspace $j \in [1, ..., n_\mathrm{A}]$, with n_A the number of considered workspaces, is discretized into a set $\mathcal{A}_j$ of up to 100 tool tip frames $A_{j,p}$ to evaluate the quality measures throughout the workspace. The orientation of these frames is chosen in a way that the z-axis is pointing opposite to the surface normal of the nearest point on the respective organ. In the following, the configuration $\mathbf{q}_{r,j,p}$ denotes the calculated joint angles of a robot r to reach a tool tip frame $A_{j,p}$.

B. Optimization Parameters

The presented design optimization incorporates both a structure synthesis to determine the general arrangement of the mechanical structure (type and number of DoF) as well as a dimensional synthesis to find optimal link lengths and joint locations[1]. To allow for freely positioning of each robot base, a total of 18 DoF would be necessary. It would however be desirable to realize a design with less actuations to reduce complexity, costs, weight, and size of the carrier. Therefore, the original design idea as depicted in Fig. 4a only disposes of 5 actuations. One goal of this study is to analyze if 5 actuations are sufficient to ensure optimal positioning of the robot bases. Fig. 4 shows all considered parameters. These parameters are combined with each other (see Sect. IV) to generate the considered design alternatives.

For every design alternative i, an optimization parameter vector is defined:

$$\mathbf{p}_i^\mathrm{T} = \left(\mathbf{p}^{\mathrm{d}\,\mathrm{T}}, \mathbf{p}_1^{\mathrm{o}\,\mathrm{T}}, ..., \mathbf{p}_j^{\mathrm{o}\,\mathrm{T}}, ..., \mathbf{p}_{n_\mathrm{A}}^{\mathrm{o}\;\mathrm{T}}\right), \tag{1}$$

and two types of optimization parameters are distinguished:

[1]A classification for optimal robot design problems is given in [9].

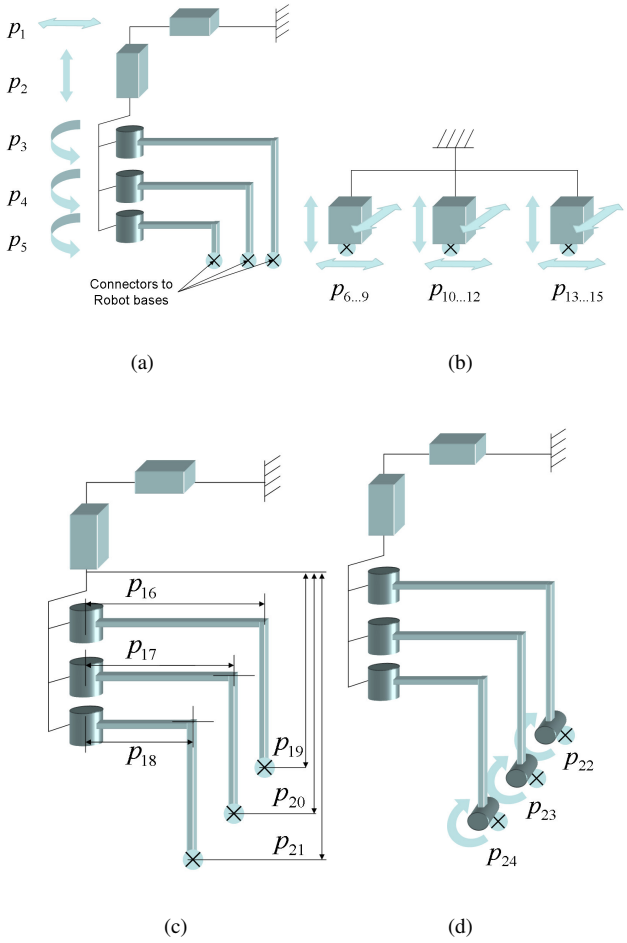

Fig. 4. Used parameters p_h in different design alternatives.

- Design parameters $\mathbf{p}^\mathrm{d}$ that are intrinsic to the design and cannot be modified once the mechanism is in use, such as e.g. segment lengths and the assembly of the actuators.
- Operation parameters $\mathbf{p}_j^\mathrm{o}$, that can be modified for every workspace j, according to a preoperative planning step, like e.g. the position of linear guides or revolutional joints.

The parameters depicted in Fig. 4 can be either design or operation parameters, depending on the resp. design alternative. Additionally, the position of the entry point into the human body is included as an operation parameter for all MIRS scenarios.

C. Evaluation Procedure

The optimization of a parameter vector $\mathbf{p}_i$ is carried out advantageously using genetic algorithms as described in [10] since in the current optimization problem the quality function is discontiguous. The adopted two-step-procedure to assign a quality value $f(\mathbf{p}_i)$ (to be minimized) is shown in Fig. 5. It integrates compulsory criteria in step one and relaxable criteria

in step two. The function $f(\mathbf{p}_i)$ yields:

$$f(\mathbf{p}_i) = \begin{cases} f^2(\mathbf{p}_i) & \text{if} \quad f_k^2(\mathbf{p}_i) < f_{k,\min}^2 \;\forall\; k\,, \\ f^1(\mathbf{p}_i) & \text{else}\,. \end{cases} \tag{2}$$

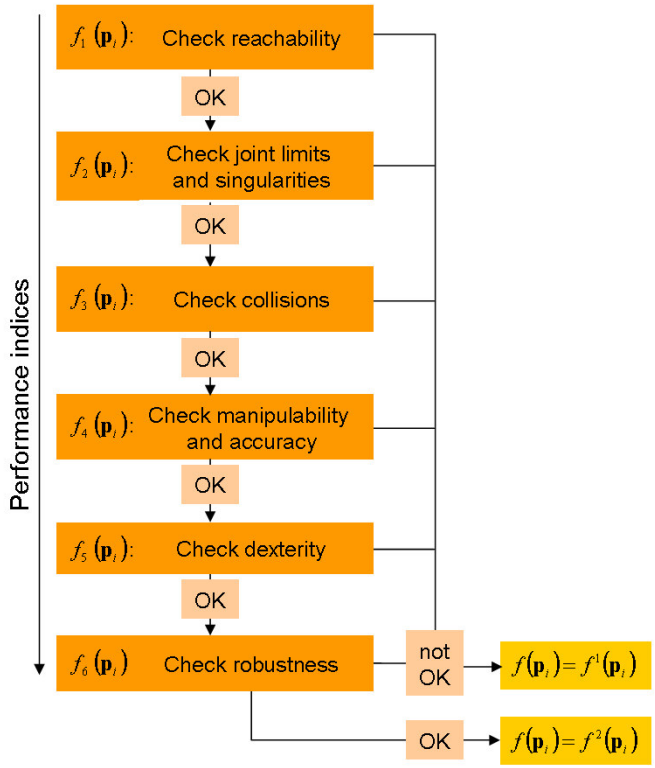

Fig. 5. Evaluation of a parameter vector $\mathbf{p}_i$.

The quality function $f^2(\mathbf{p}_i)$, upper case in (2), is chosen, provided that all minimum demands $f_{k,\min}^2$ are fulfilled. It is derived as follows: The performance index $f_k^2(\mathbf{p}_i)$ yields a quality value considering the worst occurring configuration among all quality values $f_k^2(\mathbf{p}_i, \mathbf{q}_{r,j,p})$ with respect to criterion k. In the quality function $f^2(\mathbf{p}_i)$, the performance indices $f_k^2(\mathbf{p}_i)$ are combined:

$$f^2(\mathbf{p}_i) = \left(\; f_2^2(\mathbf{p}_i) \quad , \ldots , \quad f_{n_c}^2(\mathbf{p}_i) \; \right) \mathbf{b}, \tag{3}$$

with $\mathbf{b}$ a weighting vector, n_c the number of considered criteria and $k \in [2, ..., n_c]$[2]. In case not all minimum demands $f_{k,\min}^2$ are fulfilled, the quality function $f^1(\mathbf{p}_i)$ is chosen in (2), defined as follows:

$$f^1(\mathbf{p}_i) = \frac{1}{\sum_{h=0}^{n_c-1} 10^h} \sum_{k=1}^{n_c} \left(10^{(n_c-k)} f_k^1(\mathbf{p}_i) \right) + \left(f_{2,\min}^2, \ldots, f_{n_c,\min}^2 \right) \mathbf{b}. \tag{4}$$

The performance index $f_k^1(\mathbf{p}_i) \in [0, ...1]$ expresses the rate of configurations $\mathbf{q}_{r,j,p}$ with $f_k^2(\mathbf{p}_i, \mathbf{q}_{r,j,p}) > f_{k,\min}^2$, thus violating certain minimum demands $f_{k,\min}^2$ for criterion k. In case a criterion v is violated, all performance indices $f_w^1(\mathbf{p}_i)$ with $w > v$ are set to 1 without calculation. The function $f^1(\mathbf{p}_i)$ is defined as to guarantee that $f^1(\mathbf{p}_a) > f^1(\mathbf{p}_b)$ if the index of the first violated criterion for parameter vector $\mathbf{p}_a$ is lower than for $\mathbf{p}_b$. This way, the criteria k are ordered persuant to their importance. The second term in (4) is included to ensure a continuous transition between $f^1(\mathbf{p}_i)$ and $f^2(\mathbf{p}_i)$.

The quality function $f(\mathbf{p}_i)$ has proven to be well suited for the formulation of the optimization problem, since $f^1(\mathbf{p}_i)$ enables a fast approach to good initial solutions (i.e. complying with all compulsory criteria) whereas $f^2(\mathbf{p}_i)$ allows for fine tuning of the (possibly concurring) relaxable optimization criteria. The minimization of weighted sums clearly has drawbacks as mentioned e.g. in [11]. However, in the presented method stress is laid on compliance with the compulsory requirements as shown in Tab. I, and the weighting factor $\mathbf{b}$ merely serves to explore the convex part of the Pareto curve. Note that $f_k^1(\mathbf{p}_i)$ implies also calculation of $f_k^2(\mathbf{p}_i)$, thus computation of $f^2(\mathbf{p}_i)$ is computationally cheap once $f^1(\mathbf{p}_i)$ has been calculated. Due to the use of Genetic Algorithms, the proposed optimization scheme determines a variety of alternative solutions that comply with the compulsory criteria. This may allow the designer to choose a solution that also complies with additional (not known in advance) requirements, such as e.g. installation space for the components.

The considered optimization criteria are presented below. Dynamics are not included as optimization criteria since the occurring velocities of the robotic arms remain low.

1) Reachability (f_1): Reachability is an essential criterion and therefore has the highest priority in (4). To speed up the reachability test, an analytic solution to the inverse kinematics of the KineMedic was developed, coupled with an optimization of the redundant DoF. A comparison of the calculation time and the error rate for the inverse kinematics solution of the 7−DoF KineMedic is shown in Fig. 6, considering the following algorithms (The optimization criterion for the redundant DoF is the compliance with the joint limits):

- Analytic algorithm 1: The solutions to the analytic inverse kinematics[3] are optimized subsequently with respect to the redundant DoF, using a Levenberg-Marquardt (LM) optimizer as provided in [12].
- Analytic algorithm 2: The best of all eight solutions of the analytic inverse kinematics is chosen and optimized with respect to the redundant DoF, using LM.
- Analytic algorithm 3: Joint 3 is held constant and the analytic solution is used to calculate the remaining joint angles (i.e. the robot is considered as non redundant).
- Levenberg-Marquardt algorithm: LM is used to optimize all 7 joint angles without use of an analytic solution.
- Pseudo inverse algorithm: in one-step, the solution to the inverse kinematics is approached using the pseudo inverse of the Jacobian.

[2]Reachability as expressed in criterion 1 is guaranteed for a parameter vector $\mathbf{p}_i$, if $f_1^2(\mathbf{p}_i) < f_{1,\min}^2$ and is therefore omitted in the quality function $f^2(\mathbf{p}_i)$.

[3]Note that with joint 3 held constant (non redundant case), for every tool tip frame exist 8 joint angle vectors $\mathbf{q}_{1,\ldots,8}$ that solve the inverse kinematics in case the configuration is not singular.

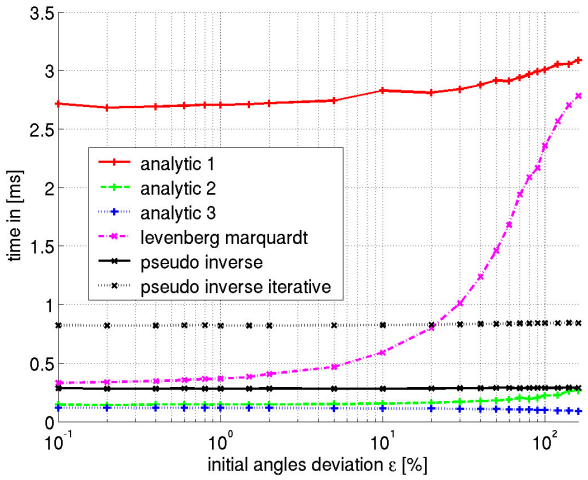

(a) Calculation time.

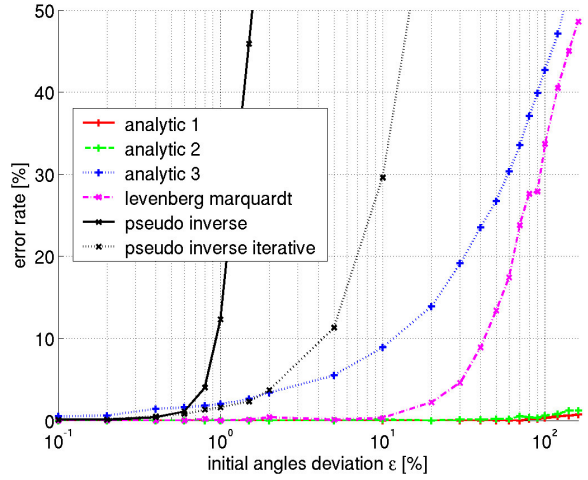

(b) Error rate.

Fig. 6. Calculation time and error rate of different inverse kinematic procedures.

- Pseudo inverse iterative algorithm: Five steps of the pseudo inverse algorithm are performed subsequently.

To calculate the error rate and the calculation speed, a set of 1000 randomly distributed reachable tool tip frames was generated and the solution of the inverse kinematics was calculated. To evaluate the influence of the deviation of the initial solution from the sought solution, the deviation ε of the initial angles $\mathbf{q}_{\text{init}}$ is plotted on the horizontal axes of Fig. 6, defined as follows:

$$\mathbf{q}_{\text{init}} = \mathbf{q}_{\text{valid}} + \text{rand} \cdot \varepsilon \left(\mathbf{q}_{\max} - \mathbf{q}_{\min} \right), \tag{5}$$

with $\mathbf{q}_{\text{valid}}$ a joint angles vector leading to the sought tool tip frame, $\text{rand} \in [0, ..., 1]$ a random number and $(\mathbf{q}_{\max}, \mathbf{q}_{\min})$ the joint limits. It can be seen from Fig. 6a that the analytic algorithm 2 is fast compared to the other algorithms and that it provides very good results even if the initial joint angles are not known (see Fig. 6b), as is the case for the current optimization. It is therefore chosen in this study.

In case of articulated instruments, first the position of the wrist and the joint angles of the instruments are calculated analytically as imposed by the tool tip position and the location of the entry point, then the joint angles of the medical robots are calculated using the analytic algorithm 2.

2) Joint Limits and Singularities (f_2): It can be shown [13] that the only singular configurations e_i of the KineMedic (inside the joint limits) are given as follows:

$$e_1: \quad q_4 = 0^\circ \quad \text{(elbow singularity)} \quad \text{and} \tag{6}$$

$$e_2: \quad q_5 = \pm 90^\circ \wedge q_6 = 0^\circ. \tag{7}$$

Thus the observance of joint limits as well as of singularities can be formulated as optimization criterion by simply regarding the minimum distance from the joint limits and the singularities among all configurations $\mathbf{q}_{r,j,p}$.

3) Collisions (f_3): In telemanipulation, collisions of the instruments should not be excluded by the system, since they are necessary and brought about by the operator to enable interaction between the tools (as e.g. in suturing tasks in medical robotics). However, collisions of the robotic arms should clearly be avoided. To save computation time, only a preliminary collision check is performed during the evaluation procedure by attaching virtual spheres S_l at the elbow (intersection of q_4 and q_5) and the wrist (intersection of q_6 and q_7) of the robot and then cross-checking the distances between every sphere l of robot r with the spheres attached to all other robots in every of their configurations k throughout the (discretized) workspace A_j. With $n_{\text{A}} = 4$ workspaces and $n_{\text{p}} = 100$ sampled points per workspace, $n_{\text{S}} = 2$ control spheres per robot and $n_{\text{R}} = 3$ robots, a total of

$$n_{\text{A}}\, n_{\text{S}}^2\, n_{\text{p}} \sum_{i=1}^{n_{\text{R}}-1} i = 4800 \tag{8}$$

distances have to be calculated. The minimum occurring distance is used as measure for collision.

4) Manipulability and Accuracy (f_4) : The criterion to take into consideration manipulability in case of a free motion of the KineMedic is defined as follows. Assuming that the robot is controlled in a way that the Euclidean norm of the occurring joint velocities is minimized, the necessary joint velocities $\dot{\mathbf{q}}$ to produce a motion $\left(\dot{\mathbf{x}}^{\text{T}}\, \boldsymbol{\omega}^{\text{T}}\right)^{\text{T}}$ can be calculated using the Moore-Penrose inverse $\mathbf{J}^+$ of the basic Jacobian $\mathbf{J}$:

$$\dot{\mathbf{q}} = \mathbf{J}^+ \begin{pmatrix} \dot{\mathbf{x}} \\ \boldsymbol{\omega} \end{pmatrix}. \tag{9}$$

The maximum occurring joint velocity $\dot{q}_{\max}^{\text{trans}}$, caused by a desired translational velocity $\|\dot{\mathbf{x}}\|_2^{\text{d}}$ of the tool tip, can be calculated from the elements $j_{i,j}^+$ of the Moore-Penrose inverse $\mathbf{J}^+$(see [14]):

$$\dot{q}_{\max}^{\text{trans}} = \max_i \sqrt{j_{i,1}^{+2} + j_{i,2}^{+2} + j_{i,3}^{+2}}\, \|\dot{\mathbf{x}}\|_2^{\text{d}}\ . \tag{10}$$

Likewise, the maximum occurring joint velocity $\dot{q}^{\mathrm{rot}}_{\max}$, caused by a desired translational velocity $\|\boldsymbol{\omega}\|^{\mathrm{d}}_2$ of the tool tip, can be calculated:

$$\dot{q}^{\mathrm{rot}}_{\max} = \max_i \sqrt{j^{+2}_{i,4} + j^{+2}_{i,5} + j^{+2}_{i,6}}\, \|\boldsymbol{\omega}\|^{\mathrm{d}}_2 \,. \qquad (11)$$

Thus the joint velocity $\dot{q}_{max} = max\,(\dot{q}^{trans}_{max},\, \dot{q}^{rot}_{max})$ can be used as measure for manipulability.

In case of a motion that is constrained due to the entry point into the human body, and for accuracy, the measure as explained in [14] is used.

5) Tool Dexterity (f_5) : The tool dexterity for articulated instruments is defined in the scope of this work as the available purely rotational motion around the target tool tip frame. This range of motion can be derived from the joint angles of the articulated instrument resp. of the joint q_7, since these joints are primarily responsible for pure rotational motion at the tool tip. The minimum distance of these joint positions from their joint limits therefore serves to formulate the criterium for dexterity.

6) Robustness (f_6): The transfer of the planned optimal setup of ports and robots into the OR introduces positioning errors, mainly due to inaccurate registration, caused by motion of the patient and organs (due to heartbeat, breathing or insufflation) and measuring faults. These errors should be reduced as far as possible, but they can never be completely eliminated. It is thus important to ensure that the operation can be carried out even if the real setup slightly deviates from the optimal setup. This is ensured by an optimization that considers also small deviations of the relevant parameters (see [15]): Both the robot base position and (for MIS) the entry points into the patient are varied successively with $\Delta p = \pm 20\mathrm{mm}$ and the optimization is rerun. Note that robustness at this point does not regard different patient anatomies but only the mentioned occurring errors in the transfer. Different patient anatomies are already taken into account at an earlier step, see III-A.

IV. Optimization Results

The underlying idea to the current study is the design of an actuated carrier for up to 3 KineMedics, mounted to the ceiling. Naturally it is not possible to evaluate every possible kinematic chain that enables the positioning of three robots in the OR. However certain design alternatives as depicted in Tab. II were optimized and compared with each other. The design alternatives are obtained by combining the parameters p_h as depicted in Fig. 4. The following results can be summarized:

- All design alternatives except for alternatives 5^* and 6^* yielded configurations that fulfill the compulsory requirements. Variation of the evaluation values is rather small, probably due to a competition between certain optimization criteria such as e.g. manipulability and accuracy.
- The design of the KineMedic was optimized for operations where it is mounted to the floor or the operating table, and resulted in an asymmetric joint range for joints 4 and 6. It was analysed if it would be advantageous to connect the instrument to the robot rotated 180 around q_6 (as has been done for all configurations in Tab. II denoted with a *) to reverse the joint limits of joint 6. However, the slight advantages in the quality measures do not justify the increased design complexity.
- Increasing the number of DoF does not significantly raise the considered quality criteria. However the design alternatives 5^* and 6^* with a reduced number of DoF yield significantly worse results. Therefore a design with 5 DoF as initially intended is approved.
- Compared to the original design, it is suggested to alter the segment lengths of the robot bases as shown in Fig. 7, Fig. 8, and Tab. III, according to the design alternative 9. First details about the design are given in [16].

TABLE II
Considered design alternatives

i	$p^{\mathrm{d}}_h,\, h=$	$p^{\mathrm{o}}_h,\, h=$	$f\,(\mathbf{p}_i)$
1	-	$\{1,...,5\}$	0.000262993
1*	-	$\{1,...,5\}$	0.000261241
2	$\{22,...,24\}$	$\{1,...,5\}$	0.000262801
2*	$\{22,...,24\}$	$\{1,...,5\}$	0.000261203
3	-	$\{6,...,15\}$	0.000261962
3*	-	$\{6,...,15\}$	0.000261041
4	$\{16,..,24\}$	$\{1,...,5\}$	0.000262793
4*	$\{16,..,24\}$	$\{1,...,5\}$	0.000260955
5*	$\{3,4,5,16,..,24\}$	$\{1,2\}$	0.000371943
6*	$\{5,16,..,24\}$	$\{1,...,4\}$	0.000298312
7*	$\{19,..,24\}$	$\{1,...,5,16,..,18\}$	0.000260928
8*	$\{16,..,21\}$	$\{1,...,5,22,..,24\}$	0.000260877
9	$\{16,..,21\}$	$\{1,...,5\}$	0.000262799

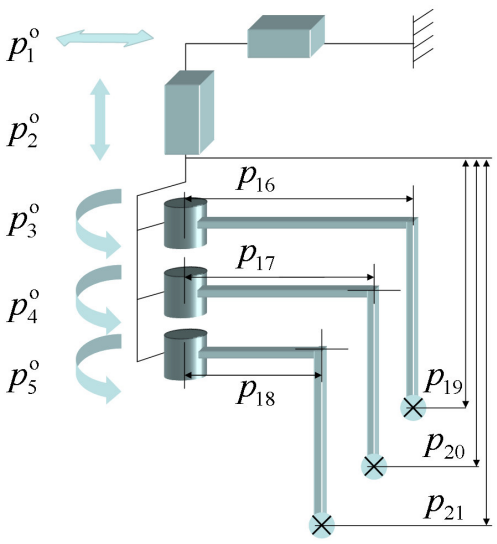

Fig. 7. Kinematic design of the suggested articulated carrier.

V. Conclusion and Outlook

Important kinematic requirements for the DLR multi-arm surgical system are developed in this paper, including relevant

TABLE III

SUGGESTED DESIGN PARAMETERS

Design parameter	Values
p^{d}_{16}	471.4 mm
p^{d}_{17}	345.9 mm
p^{d}_{18}	223.5 mm
p^{d}_{19}	7.0 mm
p^{d}_{20}	77.5 mm
p^{d}_{21}	148.1 mm

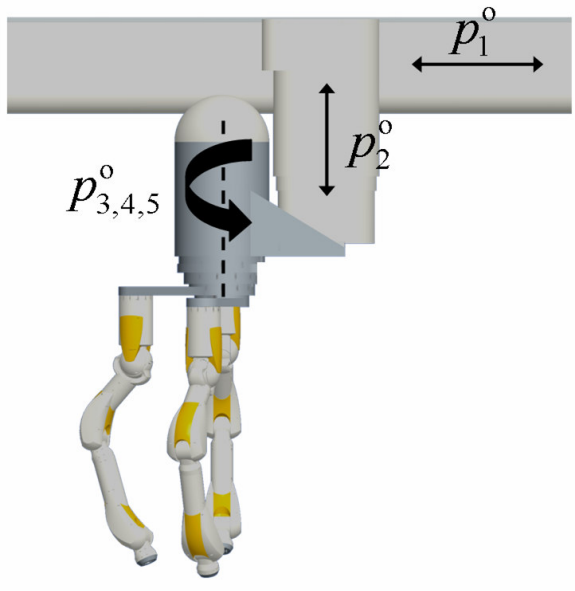

Fig. 8. Overview of the DLR medical operating scenario with the optimized actuated carrier.

workspaces and optimization criteria. An optimization procedure is presented that exploits both an analytical solution to the inverse kinematics of the KineMedic and the a priori knowledge of the singular configurations, thus augmenting calculation speed significantly. Eventually a variety of design alternatives is considered, and the choice of an actuated carrier with 5 DoF is suggested, providing a good compromise as regards sufficient dexterity and slim design. Stress is laid on the generation of a variety of design solutions, enabling the designer to choose the alternative that best fits to those criteria not be definable a priori, such as the required installation space. Furthermore, the compliance with meaningful compulsory requirements (see Tab. I) can be guaranteed. As another step in the direction of robotic assistance and autonomy functions, the integration of an automatic changing device for surgical instruments is envisaged [17]. During a MIRS intervention, the instruments are usually exchanged several times, currently manually. An automatic changing would hopefully facilitate and speed up the intervention. In terms of kinematics, it might be promising to locate the changing procedure in a space beyond the singular configurations of the medical arms, thus ensuring the space to be disjunct with the workspace of the intervention.

ACKNOWLEDGMENT

The authors would like to thank the German Academic Exchange Service, the Bavarian Research Foundation, the Bavarian Competence Network for Mechatronics, the German Research Foundation, and the company BrainLAB for their financial support. The authors appreciate the valuable comments by the anonymous reviewers, which helped strengthen the paper considerably.

REFERENCES

[1] T. Ortmaier, H. Weiß, U. Hagn, M. Nickl, A. Albu-Schäffer, C. Ott, S. Jörg, R. Konietschke, L. Le-Tien, and G. Hirzinger, "A Hands-On-Robot for Accurate Placement of Pedicle Screws," in *Proceedings of the 2006 IEEE International Conference on Robotics and Automation*, 2006.

[2] R. H. Taylor and D. Stoianovici, "Medical Robotics in Computer-Integrated Surgery," *IEEE Transactions on Robotics and Automation*, vol. 19, no. 5, pp. 765–781, 2003.

[3] Intuitive Surgical, "Company Profile – Investor Relations FAQ." [web page] `http://www.intuitivesurgical.com/`, 2005. [Accessed on 31 Jan. 2006.].

[4] È. Coste-Manière, L. Adhami, F. Mourgues, and O. Bantiche, "Optimal Planning of Robotically Assisted Heart Surgery: Transfer Precision in the Operating Room," in *8th International Symposium on Experimental Robotics (ISER)*, (Sant'Angelo d'Ischia, Italy), 2002.

[5] U. Seibold, B. Kübler, and G. Hirzinger, "Prototype of Instrument for Minimally Invasive Surgery with 6-Axis Force Sensing Capability," in *Proceedings of the 2005 IEEE International Conference on Robotics and Automation ICRA*, (Barcelona, Spain), pp. 498 – 503, 2005.

[6] R. Konietschke, H. Weiß, T. Ortmaier, and G. Hirzinger, "A Preoperative Planning Procedure for Robotically Assisted Minimally Invasive Interventions," in *3. Jahrestagung der Deutschen Gesellschaft für Computer- und Roboterassistierte Chirurgie (CURAC)*, (München, Germany), 8.-9. Dezember 2004.

[7] T. Ortmaier, *Motion Compensation in Minimally Invasive Robotic Surgery*. Munich, Germany: VDI Verlag, 2003. PhD Thesis.

[8] V. Falk, "Manual Control and Tracking – A Human Factor Analysis Relevant for Beating Heart Surgery," *Annals of Thoracic Surgery*, vol. 74, pp. 624–628, 2002.

[9] J.-P. Merlet, "Optimal Design of Robots," in *Proceedings of Robotics: Science and Systems*, (Cambridge, USA), June 2005.

[10] R. Konietschke, *Aufbauoptimierung für Roboter in medizinischen Anwendungen*. Diploma Thesis: Munich University of Technology, Germany, 2001.

[11] I. Das and J. Dennis, "A closer look at drawbacks of minimizing weighted sums of objectives for pareto set generation in multicriteria optimization problems," 1996.

[12] M. Lourakis, "levmar: Levenberg-Marquardt Nonlinear Least Squares Algorithms in C/C++." [web page] `http://www.ics.forth.gr/~lourakis/levmar/`, July 2004. [Accessed on 31 Jan. 2006.].

[13] R. Konietschke, G. Hirzinger, and Y. Yan, "All Singularities of the 9-DoF DLR Medical Robot Setup for Minimally Invasive Applications," in *Advances in Robot Kinematics*, (Ljubljana, Slovenia), 2006.

[14] R. Konietschke, T. Ortmaier, H. Weiß, G. Hirzinger, and R. Engelke, "Manipulability and Accuracy Measures for a Medical Robot in Minimally Invasive Surgery," in *Advances in Robot Kinematics*, (Genua, Italy), 2004.

[15] R. Konietschke, T. Ortmaier, H. Weiß, R. Engelke, and G. Hirzinger, "Optimal Design of a Medical Robot for Minimally Invasive Surgery," in *2. Jahrestagung der Deutschen Gesellschaft für Computer- und Roboterassistierte Chirurgie (CURAC)*, (Nürnberg, Germany), 4.-7. November 2003.

[16] S. Frumento, R. Michelini, R. Konietschke, U. Hagn, T. Ortmaier, and G. Hirzinger, "A Co-Robotic Positioning Device for Carrying Surgical End-Effectors," in *Proceedings of ESDA 2006*, (Torino, Italy), 2006.

[17] S. Frumento, *Design of Co-Robotic Devices for Minimally Invasive Robotic Surgery*. University of Genova, 2006. PhD Thesis.